

The observer's no-boundary state and axion wormholes

Erez Y. Urbach

[2505.14771] Blommaert, Kudler-Flam, EYU

[26???.?????] Blommaert, Kudler-Flam, Narovlansky, EYU

Observers, wormholes and complex saddles in cosmology, EPFL

- In AdS/CFT the holographic dual is quantum mechanical. This allowed us to learn a lot about the non-perturbative aspects of quantum gravity. Concretely, we can unambiguously define bulk operators by dressing them to the fixed conformal boundary.

Quantum gravity in closed universes

- In AdS/CFT the holographic dual is quantum mechanical. This allowed us to learn a lot about the non-perturbative aspects of quantum gravity. Concretely, we can unambiguously define bulk operators by dressing them to the fixed conformal boundary.
- For closed universes (such as de Sitter), we lack both a holographic description and a fixed boundary. It has been known for many years that in order to meaningfully define observables one needs to **introduce an ideal clock/observer** [Page-Wooters,...].

Quantum gravity in closed universes

- In AdS/CFT the holographic dual is quantum mechanical. This allowed us to learn a lot about the non-perturbative aspects of quantum gravity. Concretely, we can unambiguously define bulk operators by dressing them to the fixed conformal boundary.
- For closed universes (such as de Sitter), we lack both a holographic description and a fixed boundary. It has been known for many years that in order to meaningfully define observables one needs to **introduce an ideal clock/observer** [Page-Wooters,...].
- [Chandrasekaran, Longo, Penington & Witten, '22] Studied an ideal clock in de Sitter space at $G = 0$. This allowed them to define an (diff-invariant) **algebra of observables for the observer's static patch**.

Quantum gravity in closed universes

- In AdS/CFT the holographic dual is quantum mechanical. This allowed us to learn a lot about the non-perturbative aspects of quantum gravity. Concretely, we can unambiguously define bulk operators by dressing them to the fixed conformal boundary.
- For closed universes (such as de Sitter), we lack both a holographic description and a fixed boundary. It has been known for many years that in order to meaningfully define observables one needs to **introduce an ideal clock/observer** [Page-Wooters,...].
- [Chandrasekaran, Longo, Penington & Witten, '22] Studied an ideal clock in de Sitter space at $G = 0$. This allowed them to define an (diff-invariant) **algebra of observables for the observer's static patch**.
- The algebra was found to be type II_1 , which admits a “renormalized-entropy” function that agrees with the area law:

$$S_{\text{vN}}(\rho) = \underbrace{\frac{\delta A_{\text{dS}}}{4G}}_{\mathcal{O}(1)} + \delta S_{\text{QFT}} + C. \quad (1)$$

- In this algebra, the Hartle-Hawking/no-boundary state (Bunch-Davis) is identified with the identity operator:

$$\rho_{\text{NB}} = \mathbb{1}. \quad (2)$$

In other words, **the no-boundary state is the maximum entropy state** for the observer's algebra.

- In this algebra, the Hartle-Hawking/no-boundary state (Bunch-Davis) is identified with the identity operator:

$$\rho_{\text{NB}} = \mathbb{1}. \quad (2)$$

In other words, **the no-boundary state is the maximum entropy state** for the observer's algebra.

- **Intuition:** from the observer's perspective, the state thermalizes at late times to the Bunch-Davis state. By the second law, it is the **maximum entropy state**.

- In this algebra, the Hartle-Hawking/no-boundary state (Bunch-Davis) is identified with the identity operator:

$$\rho_{\text{NB}} = \mathbb{1}. \quad (2)$$

In other words, **the no-boundary state is the maximum entropy state** for the observer's algebra.

- **Intuition:** from the observer's perspective, the state thermalizes at late times to the Bunch-Davis state. By the second law, it is the **maximum entropy state**.
- The construction is perturbative $G \ll 1$, and allows us to only compute entropy differences from the Bunch-Davis state.

- In this algebra, the Hartle-Hawking/no-boundary state (Bunch-Davis) is identified with the identity operator:

$$\rho_{\text{NB}} = \mathbb{1}. \quad (2)$$

In other words, **the no-boundary state is the maximum entropy state** for the observer's algebra.

- **Intuition:** from the observer's perspective, the state thermalizes at late times to the Bunch-Davis state. By the second law, it is the **maximum entropy state**.
- The construction is perturbative $G \ll 1$, and allows us to only compute entropy differences from the Bunch-Davis state.
- As a result, we can't fix the additive constant in S_{vN} . More generally, unable to compare entropies around different backgrounds.

- In this algebra, the Hartle-Hawking/no-boundary state (Bunch-Davis) is identified with the identity operator:

$$\rho_{\text{NB}} = \mathbb{1}. \quad (2)$$

In other words, **the no-boundary state is the maximum entropy state** for the observer's algebra.

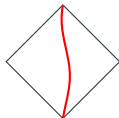
- **Intuition:** from the observer's perspective, the state thermalizes at late times to the Bunch-Davis state. By the second law, it is the **maximum entropy state**.
- The construction is perturbative $G \ll 1$, and allows us to only compute entropy differences from the Bunch-Davis state.
- As a result, we can't fix the additive constant in S_{vN} . More generally, unable to compare entropies around different backgrounds.
- We would like a "less-perturbative" principle by which we can define traces and entropies.

A background-independent algebra for observers

- [Witten '23] considered any background together with an ideal clock.

A background-independent algebra for observers

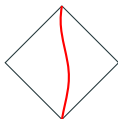
- [Witten '23] considered any background together with an ideal clock.
- One can unambiguously define an algebra for the observer's causal region.



This algebra captures all the possible experiments one can do along the clock's worldline.

A background-independent algebra for observers

- [Witten '23] considered any background together with an ideal clock.
- One can unambiguously define an algebra for the observer's causal region.

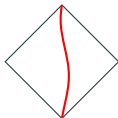


This algebra captures all the possible experiments one can do along the clock's worldline.

• **Conjecture:** ρ_{NB} is a universal maximum entropy state.

A background-independent algebra for observers

- [Witten '23] considered any background together with an ideal clock.
- One can unambiguously define an algebra for the observer's causal region.



This algebra captures all the possible experiments one can do along the clock's worldline.

Conjecture: ρ_{NB} is a universal maximum entropy state.

- This would allow us to unambiguously define entropies as

$$S(\rho) = -\langle \rho \log \rho \rangle_{\text{NB}} \equiv -S_{\text{rel}}(\rho \parallel \rho_{\text{NB}}). \quad (3)$$

Fixing the entropy's additive constant, with $C = A_{\text{dS}}/(4G)$ for dS (CLPW).

1. Give a path integral argument for Witten's conjecture for **closed universes with full causal access**.

Suggest that a Lorentzian prescription is the correct path integral definition for ρ_{NB} .

1. Give a path integral argument for Witten's conjecture for **closed universes with full causal access**.

Suggest that a Lorentzian prescription is the correct path integral definition for ρ_{NB} .

2. Test the prescription for the case of the **axion wormholes**.

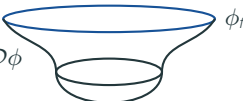
The Lorentzian contour will avoid a puzzle with the naive Euclidean prescription, and reproduce the expected answer.

The observer's no-boundary state

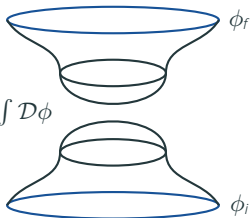
The no-boundary proposal

[Hartle, Hawking, Hertog, ...]

- For a given configuration ϕ_f , the no-boundary state $\Psi[\phi_f]$ is given by all the compact geometries that end on ϕ_f :

$$\Psi[\phi_f] = \int \mathcal{D}\phi$$
A diagram showing a compact geometry that ends on a boundary. It consists of a bowl-like shape with a circular boundary at the top, labeled ϕ_f . The interior of the bowl is shaded to represent the volume of the geometry.

- Similarly, we can write the (pure) density matrix $\rho_{\text{NB}}(\phi_f, \phi_i)$ as a path integral with two boundaries:

$$\rho_{\text{NB}}(\phi_f, \phi_i) = \int \mathcal{D}\phi$$
A diagram showing a geometry with two boundaries. It consists of two bowl-like shapes joined at their narrow ends. The top boundary is labeled ϕ_f and the bottom boundary is labeled ϕ_i . The interior of the combined shape is shaded to represent the volume of the geometry.

The observer's no-boundary state

- **With an ideal observer** (which can't annihilate), the boundary conditions include the observer's clock.

The observer's no-boundary state

- **With an ideal observer** (which can't annihilate), the boundary conditions include the observer's clock.
- For a single boundary, the observer worldline has nowhere to end:

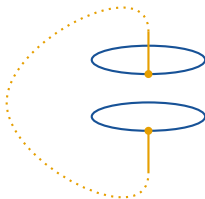


The observer's no-boundary state

- **With an ideal observer** (which can't annihilate), the boundary conditions include the observer's clock.
- For a single boundary, the observer worldline has nowhere to end:



- However for **the density matrix**, $\rho_{\text{NB}}(\phi_i, \phi_f)$, the observer worldline can start at ϕ_i and end at ϕ_f :

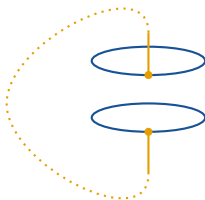


The observer's no-boundary state

- **With an ideal observer** (which can't annihilate), the boundary conditions include the observer's clock.
- For a single boundary, the observer worldline has nowhere to end:



- However for **the density matrix**, $\rho_{\text{NB}}(\phi_i, \phi_f)$, the observer worldline can start at ϕ_i and end at ϕ_f :



- Such connected geometries necessarily imply that **the observer's no-boundary state is mixed**. “bra-ket wormhole” [Page '86, Hawking '87, Chen Gorbenko Maldacena '20,.....].

The no-boundary state is the identity 1

- Including an observer, the no-boundary state between ϕ_i and ϕ_f is given by manifolds $M \times I$

$$\langle \phi_f | \rho_{NB} | \phi_i \rangle = \int \mathcal{D}\phi_{\text{bulk}} \phi_{\text{bulk}} \cdot \quad (4)$$


The diagram illustrates a manifold $M \times I$, which is a cylinder with two horizontal boundary components. The top boundary is labeled ϕ_f and the bottom boundary is labeled ϕ_i . Two paths are shown: a blue path that starts at the top boundary, goes around the cylinder, and ends at the top boundary; and a yellow path that starts at the bottom boundary, goes around the cylinder, and ends at the bottom boundary. The label ϕ_{bulk} is placed to the left of the cylinder.

The no-boundary state is the identity 1

- Including an observer, the no-boundary state between ϕ_i and ϕ_f is given by manifolds $M \times I$

$$\langle \phi_f | \rho_{NB} | \phi_i \rangle = \int \mathcal{D}\phi_{\text{bulk}} \quad \phi_{\text{bulk}} \quad \begin{array}{c} \phi_f \\ \phi_i \end{array} \quad (4)$$
A diagram of a genus-2 manifold, which is a surface with two holes. Two blue loops are drawn around the holes, representing boundary conditions ϕ_i and ϕ_f . Two orange paths are drawn on the surface, representing the bulk field configuration ϕ_{bulk} .

- This is the same path-integral used to define inner-products in the Hilbert space of closed universes!

$$\langle \phi_f | \phi_i \rangle = \int \mathcal{D}\phi_{\text{bulk}} \quad \begin{array}{c} \phi_f \\ \phi_i \end{array} \quad (5)$$
A diagram of a cylinder, representing a closed universe. Two blue horizontal lines represent the boundary conditions ϕ_i and ϕ_f . A vertical orange line with dots at its ends represents the bulk field configuration ϕ_{bulk} .

This implies that $\rho_{NB} = \mathbb{1}$.

The no-boundary state is the identity 2

- As a sanity check, we can also try to compute ρ_{NB}^2 , graphically

$$\langle \phi_f | \rho_{\text{NB}}^2 | \phi_i \rangle = \int_{\text{B.C./Diff}} \mathcal{D}\psi \quad \text{[Diagram 1]} \quad \text{[Diagram 2]}, \quad (6)$$

The diagram consists of two parts enclosed in large parentheses. The left part shows a genus-2 surface (a torus with two holes) with two blue loops labeled ϕ_f and ψ , and two green loops labeled ψ and ϕ_i . An orange path starts at a point on the top blue loop, goes around the surface, and ends at a point on the bottom green loop. The right part shows the same genus-2 surface with the same blue and green loops, but the orange path starts and ends at the same point on the top blue loop, forming a closed loop.

The no-boundary state is the identity 2

- As a sanity check, we can also try to compute ρ_{NB}^2 , graphically

$$\langle \phi_f | \rho_{\text{NB}}^2 | \phi_i \rangle = \int_{\text{B.C./Diff}} \mathcal{D}\psi \quad \left(\text{Diagram 1} \right) \quad \left(\text{Diagram 2} \right), \quad (6)$$

- Since the ψ integral is up to diff-invariance, this is the same as path-integrating over all $M \times I$ between ϕ_i and ϕ_f , which implies $\rho_{\text{NB}}^2 = \rho_{\text{NB}}$, and hence $\rho_{\text{NB}} = \mathbb{1}$ (unnormalized) on the space of physical states.

The no-boundary state is the identity 2

- As a sanity check, we can also try to compute ρ_{NB}^2 , graphically

$$\langle \phi_f | \rho_{\text{NB}}^2 | \phi_i \rangle = \int_{\text{B.C./Diff}} \mathcal{D}\psi \quad \left(\text{Diagram 1} \right) \quad \left(\text{Diagram 2} \right), \quad (6)$$


- Since the ψ integral is up to diff-invariance, this is the same as path-integrating over all $M \times I$ between ϕ_i and ϕ_f , which implies $\rho_{\text{NB}}^2 = \rho_{\text{NB}}$, and hence $\rho_{\text{NB}} = \mathbb{1}$ (unnormalized) on the space of physical states.
- Note that this is different from the Gibbs state $\rho_{\text{Gibbs}} = e^{-\beta H}$, although it has a similar path-integral description.

The no-boundary state is the identity 3

- Consider the ADM formalism, where the metric is

$$ds^2 = -N^2 dt^2 + g_{ij}(dx^i + N^i dt)(dx^j + N^j dt). \quad (7)$$

and the Einstein-Hilbert action

$$I = \int dt d^3x \left(\Pi^{ij} \dot{g}_{ij} - NH_{\text{WDW}} - \sum_i N^i P_i \right). \quad (8)$$

The no-boundary state is the identity 3

- Consider the ADM formalism, where the metric is

$$ds^2 = -N^2 dt^2 + g_{ij}(dx^i + N^i dt)(dx^j + N^j dt). \quad (7)$$

and the Einstein-Hilbert action

$$I = \int dt d^3x \left(\Pi^{ij} \dot{g}_{ij} - NH_{\text{WDW}} - \sum_i N^i P_i \right). \quad (8)$$

- For constant N minisuperspace (and $N^i = 0$), the path integral over Lorentzian $M \times I$ is

$$\langle \phi_f | \rho_{\text{NB}} | \phi_i \rangle = \langle \phi_f | \frac{1}{2\pi} \int_{-\infty}^{+\infty} dN e^{-iH_{\text{WDW}}N} | \phi_i \rangle = \langle \phi_f | \delta(H_{\text{WDW}}) | \phi_i \rangle. \quad (9)$$

The no-boundary state is the identity 3

- Consider the ADM formalism, where the metric is

$$ds^2 = -N^2 dt^2 + g_{ij}(dx^i + N^i dt)(dx^j + N^j dt). \quad (7)$$

and the Einstein-Hilbert action

$$I = \int dt d^3x \left(\Pi^{ij} \dot{g}_{ij} - NH_{\text{WDW}} - \sum_i N^i P_i \right). \quad (8)$$

- For constant N minisuperspace (and $N^i = 0$), the path integral over Lorentzian $M \times I$ is

$$\langle \phi_f | \rho_{\text{NB}} | \phi_i \rangle = \langle \phi_f | \frac{1}{2\pi} \int_{-\infty}^{+\infty} dN e^{-iH_{\text{WDW}}N} | \phi_i \rangle = \langle \phi_f | \delta(H_{\text{WDW}}) | \phi_i \rangle. \quad (9)$$

- Hence $\rho_{\text{NB}} = \delta(H_{\text{WDW}})$ is the projector onto the physical states with $H_{\text{WDW}} = 0$, which is the identity on the physical Hilbert space. **[Marolf '96, Feldbrugge Lehnert Turok '17, Banihashemi and T. Jacobson '25,...].**

$\rho_{\text{NB}} = \mathbb{1}$ is automatically implemented by the Lorentzian path integral with $-\infty < N < +\infty$.

- JT gravity is 2d dilaton gravity with the action

$$I = \frac{1}{2} \int dx \sqrt{g} \Phi (R + 2). \quad (10)$$

- JT gravity is 2d dilaton gravity with the action

$$I = \frac{1}{2} \int dx \sqrt{g} \Phi (R + 2). \quad (10)$$

- On closed slices, the gauge-fixed variables are the dilaton Φ and the scale factor α , and their conjugate momenta Π_α, Π_Φ [\[Held Maxfield '24\]](#).

- JT gravity is 2d dilaton gravity with the action

$$I = \frac{1}{2} \int dx \sqrt{g} \Phi (R + 2). \quad (10)$$

- On closed slices, the gauge-fixed variables are the dilaton Φ and the scale factor a , and their conjugate momenta Π_a, Π_Φ [Held Maxfield '24].
- The WdW Hamiltonian is $H_{\text{WdW}} = -\Pi_a \Pi_\Phi - a \Phi$. The space of physical states with $H_{\text{WdW}} = 0$ admits a complete basis:

$$\langle a, \Phi | b \rangle = \frac{1}{\sqrt{2\pi}} \frac{1}{\sqrt{a^2 - b^2}} e^{-\Phi \sqrt{a^2 - b^2}}. \quad (11)$$

for $b \in [0, \infty)$ and $\langle b_1 | b_2 \rangle = \frac{1}{b_1} \delta(b_1 - b_2)$.

- On the other hand, the no-boundary path integral gives

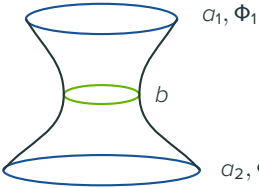
$$\langle a_1, \Phi_1 | \rho_{\text{NB}} | a_2, \Phi_2 \rangle =$$


(12)

$$= \int_0^\infty b db \langle a_1, \Phi_1 | b \rangle \langle b | a_2, \Phi_2 \rangle.$$

(13)

- On the other hand, the no-boundary path integral gives

$$\langle a_1, \Phi_1 | \rho_{\text{NB}} | a_2, \Phi_2 \rangle =$$

$$(12)$$

$$= \int_0^\infty b db \langle a_1, \Phi_1 | b \rangle \langle b | a_2, \Phi_2 \rangle .$$
$$(13)$$

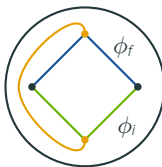
- Since the $|b\rangle$ s form a complete basis for physical states, $\rho_{\text{NB}} = \int b db |b\rangle \langle b| = \mathbb{1}$ on the physical Hilbert space.

For backgrounds with cosmological horizons, we follow the same prescription for the observer's no-boundary state.

Backgrounds with cosmological horizons

For backgrounds with cosmological horizons, we follow the same prescription for the observer's no-boundary state.

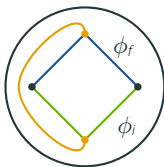
- This time, we need to specify boundary conditions for the causal diamond of the observer. The no-boundary state is given by all compact geometries that end on the observer's worldline:



Backgrounds with cosmological horizons

For backgrounds with cosmological horizons, we follow the same prescription for the observer's no-boundary state.

- This time, we need to specify boundary conditions for the causal diamond of the observer. The no-boundary state is given by all compact geometries that end on the observer's worldline:



- In de Sitter space, the no-boundary saddle is the Euclidean dS sphere, which can be thought-of as a “bra-ket wormhole” for the static patch [\[CLPW '22, Ivo Li Maldacena '24\]](#).

- By the conjecture, the entropy of the normalized no-boundary state $\tilde{\rho}_{\text{NB}}$

$$S(\tilde{\rho}_{\text{NB}}) \equiv -S_{\text{rel}}(\tilde{\rho}_{\text{NB}}||\rho_{\text{NB}}) = \log \text{tr} \rho_{\text{NB}}. \quad (14)$$

Whenever a **no-boundary geometry** \mathcal{M} **semi-classically dominate the no-boundary state**, the entropy (in this sector) is given by minus the on-shell action

$$S(\tilde{\rho}_{\text{NB}}) = \log \text{tr} \rho_{\text{NB}} = -I_{\mathcal{M}} + O(1). \quad (15)$$

In general, this is **not the area law**.

- By the conjecture, the entropy of the normalized no-boundary state $\tilde{\rho}_{\text{NB}}$

$$S(\tilde{\rho}_{\text{NB}}) \equiv -S_{\text{rel}}(\tilde{\rho}_{\text{NB}} || \rho_{\text{NB}}) = \log \text{tr} \rho_{\text{NB}}. \quad (14)$$

Whenever a **no-boundary geometry** \mathcal{M} **semi-classically dominate the no-boundary state**, the entropy (in this sector) is given by minus the on-shell action

$$S(\tilde{\rho}_{\text{NB}}) = \log \text{tr} \rho_{\text{NB}} = -I_{\mathcal{M}} + O(1). \quad (15)$$

In general, this is **not the area law**.

- As in CLPW, we expect the algebra in those cases to be type II. However, for a general no-boundary background (lacking a timelike isometry) it is not clear how to construct it.

The $D = 3$ de Sitter axion wormhole

[Myers '88, Aguilar-Gutierrez, Hertog, Tielemans, van der Schaar, Van Riet '23]

- Consider $D = 3$ gravity with a $\Lambda > 0$ together with an axion flux density ($H = 1$) $Q = q(16\pi G)^{-1/2}$ with $0 \leq q \leq 1$. We look for an FLRW solution

$$ds^2 = -dt^2 + a(t)^2 d\Omega_2^2, \quad d\Omega_2^2 = d\theta^2 + \sin^2 \theta d\phi^2. \quad (16)$$

[Myers '88, Aguilar-Gutierrez, Hertog, Tielemans, van der Schaar, Van Riet '23]

- Consider $D = 3$ gravity with a $\Lambda > 0$ together with an axion flux density ($H = 1$) $Q = q(16\pi G)^{-1/2}$ with $0 \leq q \leq 1$. We look for an FLRW solution

$$ds^2 = -dt^2 + a(t)^2 d\Omega_2^2, \quad d\Omega_2^2 = d\theta^2 + \sin^2 \theta d\phi^2. \quad (16)$$

- The solution is

$$a^2(t) = \frac{1 + \sqrt{1 - q^2} \cosh(2t)}{2}. \quad (17)$$

[Myers '88, Aguilar-Gutierrez, Hertog, Tielemans, van der Schaar, Van Riet '23]

- Consider $D = 3$ gravity with a $\Lambda > 0$ together with an axion flux density ($H = 1$) $Q = q(16\pi G)^{-1/2}$ with $0 \leq q \leq 1$. We look for an FLRW solution

$$ds^2 = -dt^2 + a(t)^2 d\Omega_2^2, \quad d\Omega_2^2 = d\theta^2 + \sin^2 \theta d\phi^2. \quad (16)$$

- The solution is

$$a^2(t) = \frac{1 + \sqrt{1 - q^2} \cosh(2t)}{2}. \quad (17)$$

- $q = 0$: dS $a(t) = \cosh(t)$.
- $q = 1$: Einstein's static universe $a^2(t) = 1/2$.

[Myers '88, Aguilar-Gutierrez, Hertog, Tielemans, van der Schaar, Van Riet '23]

- Consider $D = 3$ gravity with a $\Lambda > 0$ together with an axion flux density ($H = 1$) $Q = q(16\pi G)^{-1/2}$ with $0 \leq q \leq 1$. We look for an FLRW solution

$$ds^2 = -dt^2 + a(t)^2 d\Omega_2^2, \quad d\Omega_2^2 = d\theta^2 + \sin^2 \theta d\phi^2. \quad (16)$$

- The solution is

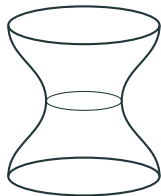
$$a^2(t) = \frac{1 + \sqrt{1 - q^2} \cosh(2t)}{2}. \quad (17)$$

- $q = 0$: dS $a(t) = \cosh(t)$.
- $q = 1$: Einstein's static universe $a^2(t) = 1/2$.
- The solution is asymptotically de Sitter for $|t| \gg 1$.

- In Euclidean signature $t = i\tau$, the solution is

$$a^2(\tau) = \frac{1 + \sqrt{1 - q^2} \cos(2\tau)}{2}. \quad (18)$$

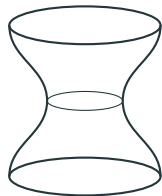
The solution starts at $\tau = 0$ with $a_{\max}^2 = \frac{1 + \sqrt{1 - q^2}}{2}$, reaches its minimal size $a_{\min}^2 = \frac{1 - \sqrt{1 - q^2}}{2}$ at $\tau = \pi/2$ and then grows back to a_{\max} at $\tau = \pi$:



- In Euclidean signature $t = i\tau$, the solution is

$$a^2(\tau) = \frac{1 + \sqrt{1 - q^2} \cos(2\tau)}{2}. \quad (18)$$

The solution starts at $\tau = 0$ with $a_{\max}^2 = \frac{1 + \sqrt{1 - q^2}}{2}$, reaches its minimal size $a_{\min}^2 = \frac{1 - \sqrt{1 - q^2}}{2}$ at $\tau = \pi/2$ and then grows back to a_{\max} at $\tau = \pi$:



- This is a **no-boundary wormhole geometry**, with an on-shell action

$$h_1 = -\pi(1 - q)/(2G). \quad (19)$$

- **“Necklaces”**: since the Euclidean solution is periodic $\tau \sim \tau + \pi$, we can glue k copies of the solution together:



Axion wormholes: the puzzle

- “**Necklaces**”: since the Euclidean solution is periodic $\tau \sim \tau + \pi$, we can glue k copies of the solution together:



- Taking $0 \leq \tau \leq \mathbf{N}_k = \pi \mathbf{k}$ for integer k gives a no-boundary saddle with on-shell action $I_k = k \cdot I_1$.

- “**Necklaces**”: since the Euclidean solution is periodic $\tau \sim \tau + \pi$, we can glue k copies of the solution together:



- Taking $0 \leq \tau \leq \mathbf{N}_k = \pi \mathbf{k}$ for integer k gives a no-boundary saddle with on-shell action $I_k = k \cdot I_1$.
- Since all the necklaces satisfy the same boundary conditions, in any sensible Euclidean prescription for ρ_{NB} we need to sum over all of them, which gives an unbounded answer!

$$\rho_{\text{NB}} \sim \sum_k^{\infty} e^{k \cdot |I_1|} = \infty. \quad (20)$$

Axion wormholes: the puzzle

- **“Necklaces”**: since the Euclidean solution is periodic $\tau \sim \tau + \pi$, we can glue k copies of the solution together:



- Taking $0 \leq \tau \leq \mathbf{N}_k = \pi \mathbf{k}$ for integer k gives a no-boundary saddle with on-shell action $I_k = k \cdot I_1$.
- Since all the necklaces satisfy the same boundary conditions, in any sensible Euclidean prescription for ρ_{NB} we need to sum over all of them, which gives an unbounded answer!

$$\rho_{\text{NB}} \sim \sum_k^{\infty} e^{k \cdot |I_1|} = \infty. \quad (20)$$

- **This is the dS axion wormhole puzzle we would like to address.**

- In order to address the puzzle in a tractable way, we performed a **truncation to minisuperspace** [Halliwell Myers '89].
[Dorronsoro,Halliwell,Hartle,Hertog,Janssen '17]

- In order to address the puzzle in a tractable way, we performed a **truncation to minisuperspace** [Halliwell Myers '89].
[Dorronsoro, Halliwell, Hartle, Hertog, Janssen '17]
- Concretely, we freeze the degrees of freedom of the axion (fix q), and consider a **constant lapse** N and a **homogeneous scale factor** $a(t)$:

$$ds^2 = N^2 d\tau^2 + a(\tau)^2 d\Omega_2^2. \quad (21)$$

- In order to address the puzzle in a tractable way, we performed a **truncation to minisuperspace** [Halliwell Myers '89].
[Dorronsoro, Halliwell, Hartle, Hertog, Janssen '17]
- Concretely, we freeze the degrees of freedom of the axion (fix q), and consider a **constant lapse** N and a **homogeneous scale factor** $a(t)$:

$$ds^2 = N^2 d\tau^2 + a(\tau)^2 d\Omega_2^2. \quad (21)$$

- The Euclidean action

$$I_E[a(t), N] = \frac{1}{2G} \int_0^N d\tau \left(-\dot{a}^2 + a^2 - 1 + \frac{q^2}{4a^2} \right). \quad (22)$$

- In order to address the puzzle in a tractable way, we performed a **truncation to minisuperspace** [Halliwell Myers '89].
[Dorronsoro, Halliwell, Hartle, Hertog, Janssen '17]
- Concretely, we freeze the degrees of freedom of the axion (fix q), and consider a **constant lapse** N and a **homogeneous scale factor** $a(t)$:

$$ds^2 = N^2 d\tau^2 + a(\tau)^2 d\Omega_2^2. \quad (21)$$

- The Euclidean action

$$I_E[a(t), N] = \frac{1}{2G} \int_0^N d\tau \left(-\dot{a}^2 + a^2 - 1 + \frac{q^2}{4a^2} \right). \quad (22)$$

- Note that the action has an $a \mapsto -a$ symmetry. Since the metric is identified under $a \mapsto -a$, we need to **gauge this symmetry**.

The no-boundary density matrix

- The matrix element of the no-boundary state between two scale factors a_1 and a_2 is given by

$$\langle a_1 | \rho_{\text{NB}} | a_2 \rangle = \int_C dN \tilde{\mathcal{G}}(a_1, a_2; N), \quad (23)$$

The no-boundary density matrix

- The matrix element of the no-boundary state between two scale factors a_1 and a_2 is given by

$$\langle a_1 | \rho_{\text{NB}} | a_2 \rangle = \int_C dN \tilde{\mathcal{G}}(a_1, a_2; N), \quad (23)$$

- Due to the $a \mapsto -a$ gauging, the propagator is actually a sum of two standard propagators:

$$\tilde{\mathcal{G}}(a_1, a_2; N) = \mathcal{G}(a_1, a_2; N) + \mathcal{G}(a_1, -a_2; N), \quad (24)$$

The no-boundary density matrix

- The matrix element of the no-boundary state between two scale factors a_1 and a_2 is given by

$$\langle a_1 | \rho_{\text{NB}} | a_2 \rangle = \int_C dN \tilde{\mathcal{G}}(a_1, a_2; N), \quad (23)$$

- Due to the $a \mapsto -a$ gauging, the propagator is actually a sum of two standard propagators:

$$\tilde{\mathcal{G}}(a_1, a_2; N) = \mathcal{G}(a_1, a_2; N) + \mathcal{G}(a_1, -a_2; N), \quad (24)$$

- Each propagator satisfies $\nu = \sqrt{\frac{1}{4} - \frac{q^2}{4G^2}}$

$$\mathcal{G}(a_1, a_2; N) = \int_{a(0)=a_1}^{a(N)=a_2} \mathcal{D}a(\tau) \exp(-I_E[a(\tau), N]) \quad (25)$$

$$= \frac{2\sqrt{-a_1 a_2}}{\sin(N)} \exp\left\{ \frac{N}{2G} + \frac{(a_1^2 + a_2^2)}{2G \tan(N)} \right\} K_\nu\left(\frac{a_1 a_2}{G \sin(N)} \right). \quad (26)$$

$$\tilde{\mathcal{G}}(a_1, a_2; N) = \mathcal{G}(a_1, a_2; N) + \mathcal{G}(a_1, -a_2; N) \quad (27)$$

- In the semiclassical limit $G \ll 1$, each propagator \mathcal{G}_{\pm} is dominated by a classical solution $a_{\pm, N}(t)$.

$$\tilde{\mathcal{G}}(a_1, a_2; N) = \mathcal{G}(a_1, a_2; N) + \mathcal{G}(a_1, -a_2; N) \quad (27)$$

- In the semiclassical limit $G \ll 1$, each propagator \mathcal{G}_{\pm} is dominated by a classical solution $a_{\pm, N}(t)$.
- For simplicity (and I'm probably out of time)

$$\tilde{\mathcal{G}}(a_1, a_2; N) = \mathcal{G}(a_1, a_2; N) + \mathcal{G}(a_1, -a_2; N) \quad (27)$$

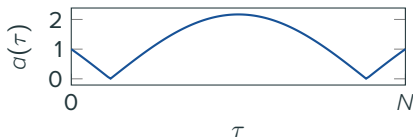
- In the semiclassical limit $G \ll 1$, each propagator \mathcal{G}_{\pm} is dominated by a classical solution $a_{\pm, N}(t)$.
- For simplicity (and I'm probably out of time)
 1. Take the smooth pure gravity limit $q \rightarrow 0$. In this limit the $a = 0$ point is a "brick wall" due to the flux potential.

$$\tilde{\mathcal{G}}(a_1, a_2; N) = \mathcal{G}(a_1, a_2; N) + \mathcal{G}(a_1, -a_2; N) \quad (27)$$

- In the semiclassical limit $G \ll 1$, each propagator \mathcal{G}_{\pm} is dominated by a classical solutions $a_{\pm, N}(t)$.
- For simplicity (and I'm probably out of time)
 1. Take the smooth pure gravity limit $q \rightarrow 0$. In this limit the $a = 0$ point is a "brick wall" due to the flux potential.
 2. Set $a_1 = a_2 = 1$.

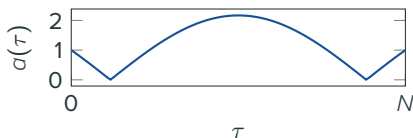
- The $a_1 \mapsto a_2$ sector is dominated in the $G \ll 1$ limit by the solution ($0 \leq \tau \leq N$)

$$a(\tau) = \left| \frac{\cos(N/2 - \tau)}{\cos(N/2)} \right|. \quad (28)$$



- The $\alpha_1 \mapsto \alpha_2$ sector is dominated in the $G \ll 1$ limit by the solution ($0 \leq \tau \leq N$)

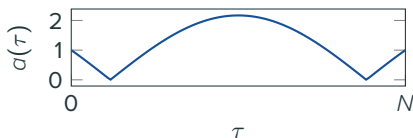
$$a(\tau) = \left| \frac{\cos(N/2 - \tau)}{\cos(N/2)} \right|. \quad (28)$$



- $N_{2m} = 2m \cdot \pi$, is the **(2m)-necklace**.
The solution **diverges** for odd $N_{2m+1} = (2m + 1) \cdot \pi$.

- The $\alpha_1 \mapsto \alpha_2$ sector is dominated in the $G \ll 1$ limit by the solution ($0 \leq \tau \leq N$)

$$a(\tau) = \left| \frac{\cos(N/2 - \tau)}{\cos(N/2)} \right|. \quad (28)$$



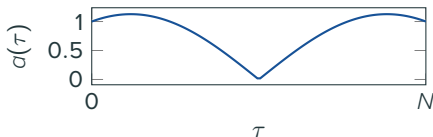
- $N_{2m} = 2m \cdot \pi$, is the **(2m)-necklace**.
The solution **diverges** for odd $N_{2m+1} = (2m + 1) \cdot \pi$.
- The on-shell action is

$$l^{(+)}(N) = \frac{1}{2G} (-N + 2 \tan(N/2)). \quad (29)$$

N_{2m} are saddles of the action with $l = 2m \cdot l_1$, while N_{2m+1} are poles of $l^{(+)}(N)$.

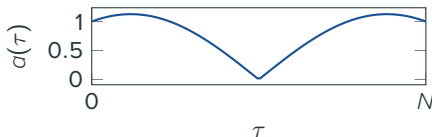
- The $a_1 \mapsto -a_2$ sector is dominated in the $G \ll 1$ limit by the solution ($0 \leq \tau \leq N$)

$$a(\tau) = \left| \frac{\sin(N/2 - \tau)}{\sin(N/2)} \right|. \quad (30)$$



- The $a_1 \mapsto -a_2$ sector is dominated in the $G \ll 1$ limit by the solution ($0 \leq \tau \leq N$)

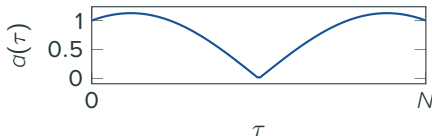
$$a(\tau) = \left| \frac{\sin(N/2 - \tau)}{\sin(N/2)} \right|. \quad (30)$$



- $N_{2m+1} = (2m + 1) \cdot \pi$ is the $(2m + 1)$ -**necklace**.
The solution **divrges** for even $N_{2m} = 2m \cdot \pi$.

- The $a_1 \mapsto -a_2$ sector is dominated in the $G \ll 1$ limit by the solution ($0 \leq \tau \leq N$)

$$a(\tau) = \left| \frac{\sin(N/2 - \tau)}{\sin(N/2)} \right|. \quad (30)$$



- $N_{2m+1} = (2m + 1) \cdot \pi$ is the **(2m + 1)-necklace**.
The solution **diverges** for even $N_{2m} = 2m \cdot \pi$.
- The on-shell action is

$$l^{(-)}(N) = \frac{1}{2G} (-N - 2 \cot(N/2)). \quad (31)$$

N_{2m+1} are saddles of the action with $l = (2m + 1) \cdot l_1$, while N_{2m} are poles of $l^{(-)}(N)$.

Specifically, $l^{(-)}(N)$ has a pole at $N = 0$! ($k = 0$)

- In the semiclassical limit, we found

$$\langle a_1 | \rho_{\text{NB}} | a_2 \rangle \sim \int_{\mathcal{C}} dN \left(e^{-I^{(+)}(N)} + e^{-I^{(-)}(N)} \right). \quad (32)$$

- In the semiclassical limit, we found

$$\langle a_1 | \rho_{\text{NB}} | a_2 \rangle \sim \int_{\mathcal{C}} dN \left(e^{-I^{(+)}(N)} + e^{-I^{(-)}(N)} \right). \quad (32)$$

All the k -necklaces appear as saddles of either $I^{(\pm)}$.

- In the semiclassical limit, we found

$$\langle a_1 | \rho_{\text{NB}} | a_2 \rangle \sim \int_{\mathcal{C}} dN \left(e^{-I^{(+)}(N)} + e^{-I^{(-)}(N)} \right). \quad (32)$$

All the k -necklaces appear as saddles of either $I^{(\pm)}$.

- **What is the correct lapse contour \mathcal{C} ?**

We would like to take the pure Lorentzian contour $\mathcal{C} = i\mathbb{R}$. However, the action has a pole on the contour at $N = 0$!

- In the semiclassical limit, we found

$$\langle \alpha_1 | \rho_{\text{NB}} | \alpha_2 \rangle \sim \int_{\mathcal{C}} dN \left(e^{-I^{(+)}(N)} + e^{-I^{(-)}(N)} \right). \quad (32)$$

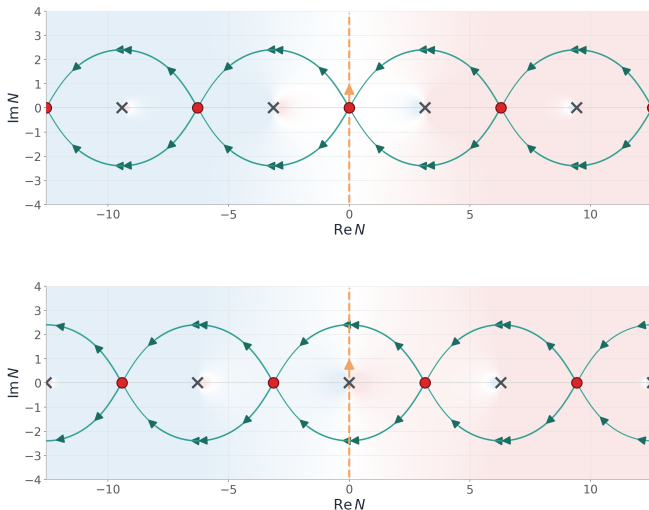
All the k -necklaces appear as saddles of either $I^{(\pm)}$.

- **What is the correct lapse contour \mathcal{C} ?**

We would like to take the pure Lorentzian contour $\mathcal{C} = i\mathbb{R}$. However, the action has a pole on the contour at $N = 0$!

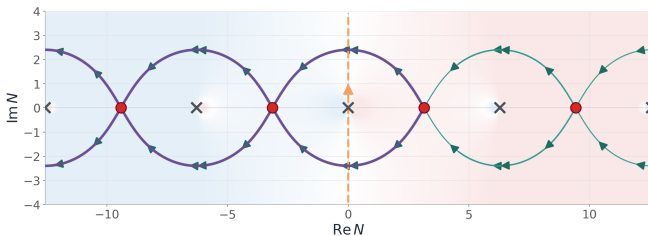
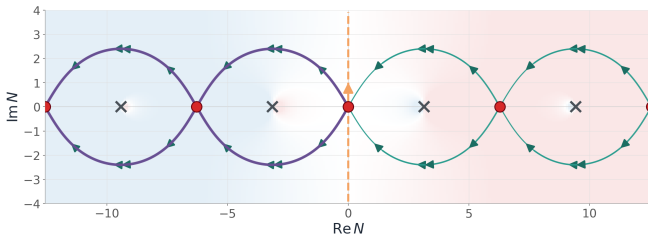
- Two options [**Hartle, Hawking, Vilenkin, Halliwell, Feldbrugge, Lehnert, Turok...**]:
 1. Deform to the right $\mathcal{C} = i\mathbb{R} + \varepsilon$ - “Hartle-Hawking”
Similar to the $i\varepsilon$ prescription in QFT!
 2. Deform to the left $\mathcal{C} = i\mathbb{R} - \varepsilon$ - “Vilenkin”
Treats gravitational saddles as instantons.

Steepest descent analysis: + (top) and - (bottom) sectors



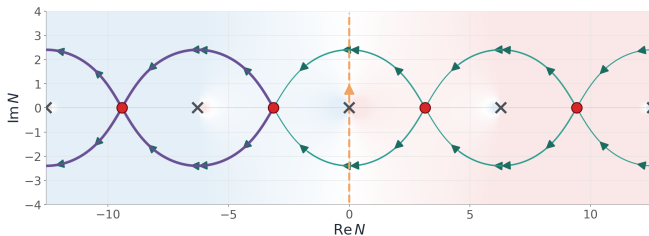
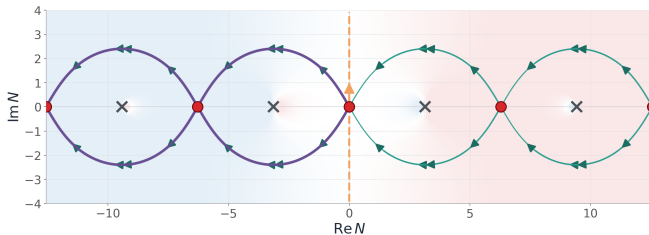
Arrows in the direction that decreases $\text{Re}l(N)$. Saddle in red, poles in "x".

Deform to the right $\mathcal{C} = i\mathbb{R} + \varepsilon$



Purple is the steepest descent contour. Collect only N_k saddles with $k \leq 1$!

Deform to the left $\mathcal{C} = i\mathbb{R} - \varepsilon$



Purple is the steepest descent contour. Collect only N_k saddles with $k \leq 0$!

- For both choices of a Lorentzian contour, the deformation to steepest descent lines avoids the divergent sum over large $k \gg 1$ necklaces!

The Lorentzian contour avoids the divergent sum!

- For both choices of a Lorentzian contour, the deformation to steepest descent lines avoids the divergent sum over large $k \gg 1$ necklaces!

The Lorentzian contour avoids the divergent sum!

- When we **deform to the right** $\mathcal{C} = i\mathbb{R} + \varepsilon$, the steepest descent contour picks the leading $k = 1$ saddle with a negative action.
Gives tree-level entropy

$$S = -h_1 = \pi(1 - q)/2G + \dots \quad (33)$$

In the dS $q = 0$ limit, we recover the area law.

- For both choices of a Lorentzian contour, the deformation to steepest descent lines avoids the divergent sum over large $k \gg 1$ necklaces!

The Lorentzian contour avoids the divergent sum!

- When we **deform to the right** $\mathcal{C} = i\mathbb{R} + \varepsilon$, the steepest descent contour picks the leading $k = 1$ saddle with a negative action.
Gives tree-level entropy

$$S = -h_1 = \pi(1 - q)/2G + \dots \quad (33)$$

In the dS $q = 0$ limit, we recover the area law.

- When we **deform to the left** $\mathcal{C} = i\mathbb{R} - \varepsilon$, the steepest descent contour picks, to leading order, the $k = 0$ saddles with zero action and thus entropy

$$S \sim O(1). \quad (34)$$

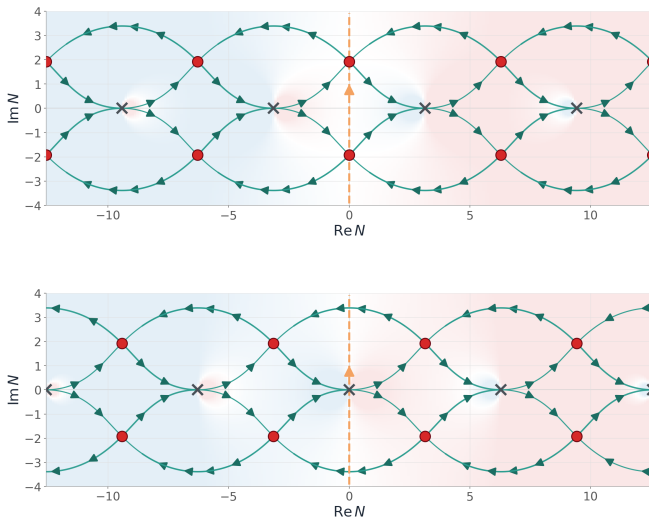
Summary

1. Provided a **path-integral evidence** for the $\rho_{\text{NB}} = \mathbb{1}$ conjecture.
2. Consistent with CLPW for dS and $\Lambda < 0$ JT gravity.
3. Whenever semiclassical approximations apply, suggests “**entropy = -action**”.
4. Suggest that the no-boundary state is defined via a Lorentzian prescription.
5. Such prescription solves the “necklace puzzle” for $D = 3$ axion wormholes.

Future directions

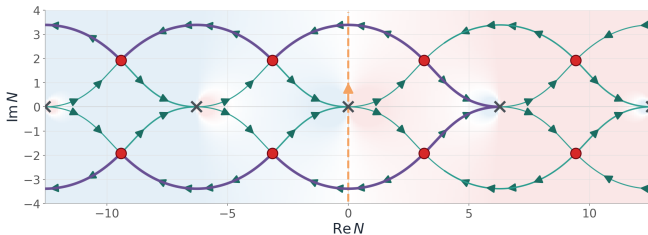
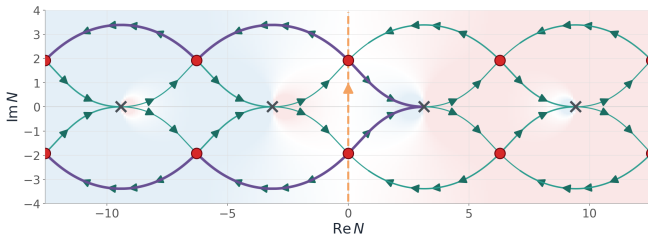
1. Other entropic puzzles?
2. How to see the transition from type II at $q = 0$ to type I at $q = 1$?
3. How to build the observer’s type II algebra for other asymptotically dS backgrounds? [**Speranza, in 1m**]
4. Add quantum corrections, a less ideal clock? [**Kolchmeyer, afternoon**]

Steepest descent analysis: + (top) and - (bottom) sectors



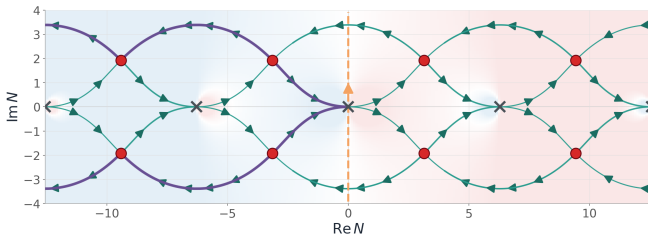
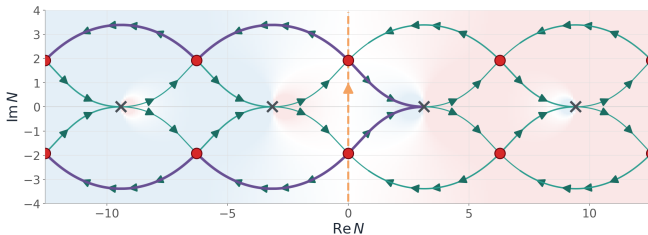
Arrows in the direction that decreases $\text{Re } l(N)$. Saddle in red, poles in "x".

Deform to the right $\mathcal{C} = i\mathbb{R} + \varepsilon$



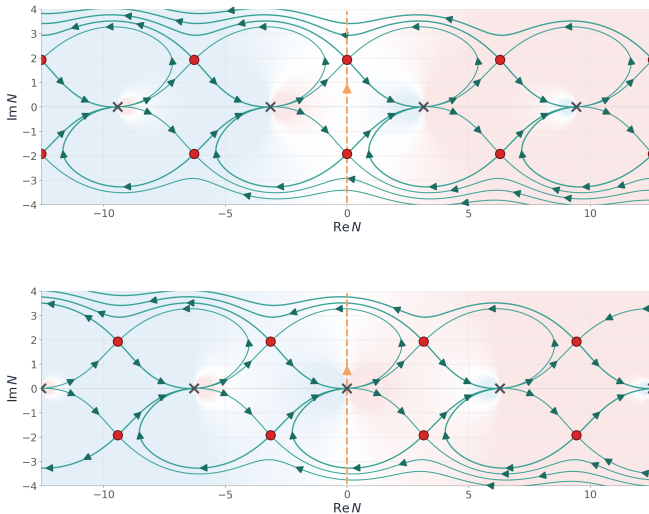
Purple is the steepest descent contour. Collect only N_k saddles with $k \leq 1$!

Deform to the left $\mathcal{C} = i\mathbb{R} - \varepsilon$



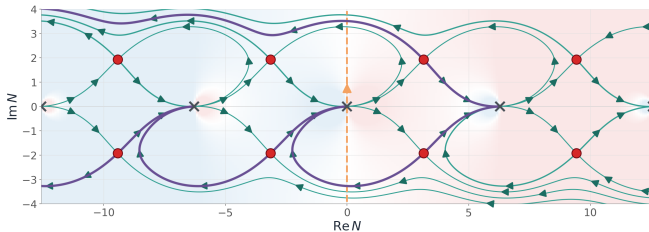
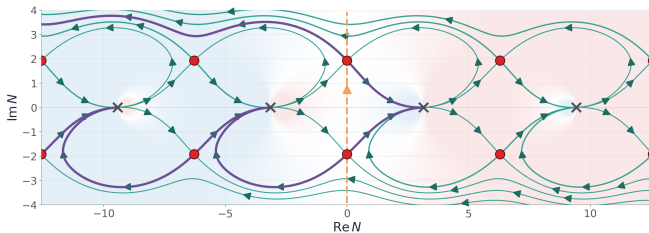
Purple is the steepest descent contour. Collect only N_k saddles with $k \leq 0$!

Steepest descent analysis with ε : + (top) and - (bottom) sectors



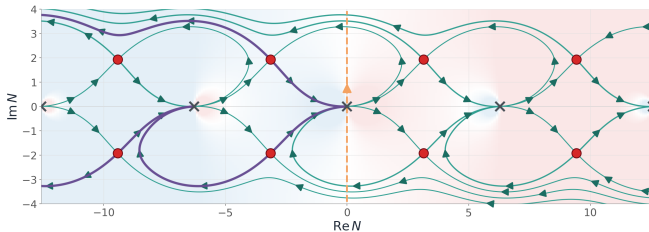
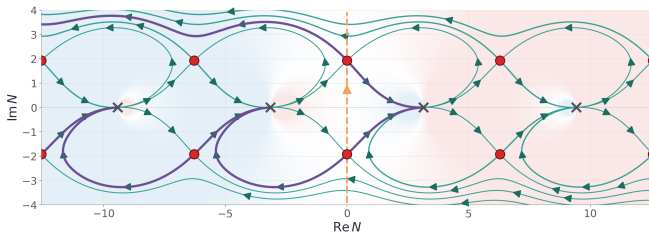
Arrows in the direction that decreases $\text{Re } l(N)$. Saddle in red, poles in "x".

With ε : deform to the right



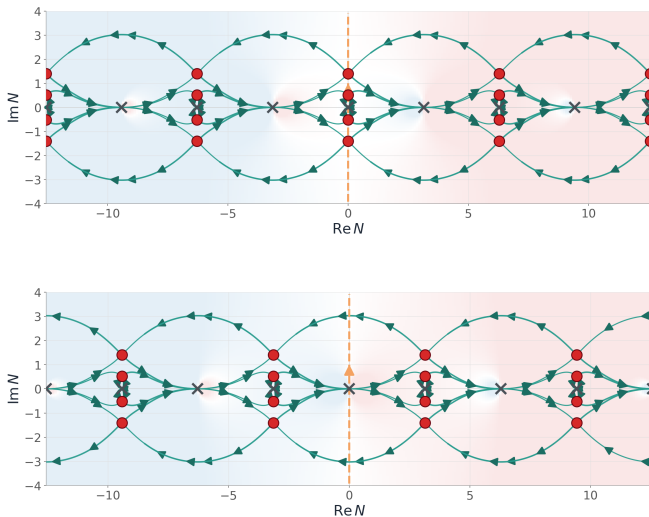
Purple is the steepest descent contour. Collect only N_k saddles with $k \leq 1$!

With ε : deform to the left



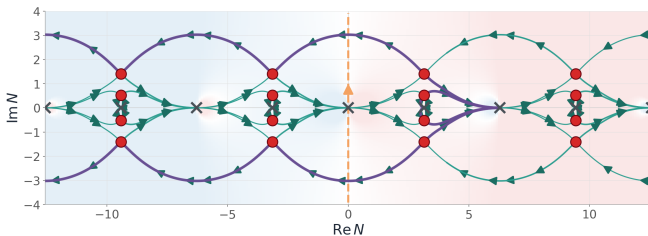
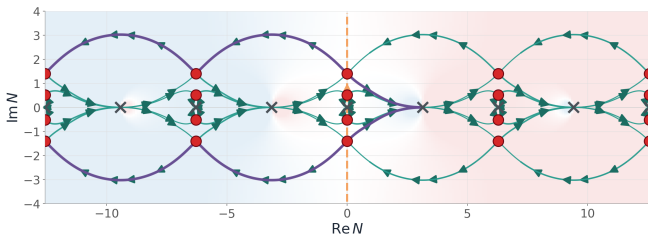
Purple is the steepest descent contour. Collect only N_k saddles with $k \leq 0$!

Steepest descent analysis, off-diagonal: + (top) and - (bottom) sectors



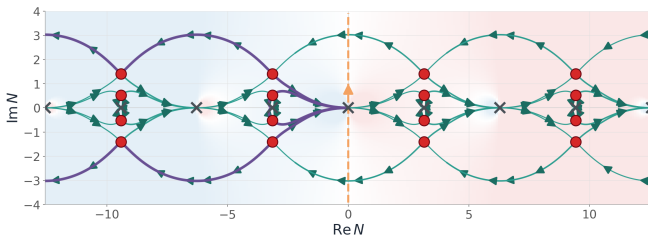
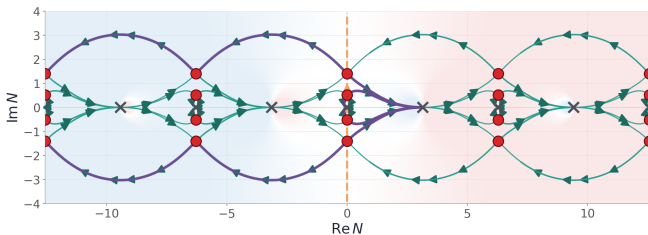
Arrows in the direction that decreases $\text{Re} l(N)$. Saddle in red, poles in “x”.

Off-diagonal: deform to the right



Purple is the steepest descent contour. Collect only N_k saddles with $k \leq 1$!

Off-diagonal: deform to the left



Purple is the steepest descent contour. Collect only N_k saddles with $k \leq 0$!